

Improvement of a Code-Based Kartini Reactor Simulator for Education and Training

Sutanto^{a,*}, Intan Nafisah^a, Anhar R. Antariksawan^b, Jianhui Wu^c

^a*Polytechnic Institute of Nuclear Technology, Babarsari Street, Yogyakarta, Indonesia*

^b*Center for Research of Accelerator Technology-National Innovation and Research Agency, Babarsari Street, Yogyakarta, Indonesia*

^c*Center for Thorium Molten Salt Reactor System, Shanghai Institute of Applied Physics, Chinese Academy of Science, Jiading Campus, Shanghai, P.R. China*

Corresponding author: *suta012@brin.go.id

Abstract—A code-based Kartini reactor simulator was improved as a facility for the human resource development of a nuclear reactor. The simulator simulates the plant dynamics regarding a change of a control rod position. Reactor operation parameter calculations of the reactor power, coolant flow, and fuel temperatures adopt a one-channel method with assumptions of homogeneous radial power distribution and a cosine function of the axial power distribution. Point reactor kinetics, radial conduction heat transfer, and mass and energy conservation are the calculation code's governing equations. Reactivity feedback due to the coolant density and fuel temperature changes are considered. Reactor pressure is fixed at 1 atm due to an open pool-type research reactor. A graphical user interface was developed to operate the simulator. The operation results of the simulator show that the power calculation agrees well with the experimental data. An accident of excess reactivity due to a control ejection is assumed to happen, causing a positive reactivity insertion of 1.11\$. However, the safety criterion of the cladding temperature is satisfied due to the negative reactivity feedback. Besides, early application of 3D virtual reality was carried out to provide an immersive interaction between the users and the virtual Kartini reactor plant. The further development of integrating both the virtual reality and the simulator in the recent Kartini reactor-based internet reactor laboratory is interesting to provide a facility with features of remote as well as immersive education and training.

Keywords—Reactor simulator; education and training, emergency condition, virtual reality.

*Manuscript received 31 Aug. 2022; revised 7 Nov. 2022; accepted 7 May 2023. Date of publication 31 Aug. 2023.
IJASEIT is licensed under a Creative Commons Attribution-Share Alike 4.0 International License.*



I. INTRODUCTION

Experiences of the past three major reactor accidents of TMI-2 (1979), Chernobyl (1986), and Fukushima Daiichi (2011) have given a lesson learned of the potential hazard of long-term radiation exposure to the surrounding environment [1]–[3]. Since that, strict safety standards have been applied in nuclear-related activities. To avoid direct radiation exposure, reactor simulators have played important roles in nuclear activities, such as reactor design, safety analysis, conducting nuclear facility tests, and educating and training nuclear reactor personnel [4]–[7]. Well-trained reactor operators will determine the safe and efficient operation of nuclear power plants, and it is not an option to conduct the training using a real nuclear power reactor. Meanwhile, a target of zero carbon emission in 2060 might encourage the use of more nuclear power plants in the future [8], [9]. Given its technology, developments of new concepts of nuclear

power reactors require computer-based codes for reactor design and safety analyses [10]–[12].

A long-term experience in the development and operation of nuclear reactors in the world has pushed many applications of computer-based reactor simulation for reactor research and for education and training [13], [14]. A computer code validated experimentally was used to determine the specific dimension of coolant flow channels of a generation-IV sodium-cooled fast power reactor [10]. It relates to satisfying the desired flow distribution for cooling the reactor core. A point neutronic calculation model is useful for analyzing a specific case of a power reactor system. In a large-scale system, a 3D neutronic calculation model was developed to analyze the plant system [15] more accurately. Using a 3D model applied in an established VVER-1000 NESTLE code also enhances the calculation of the spent nuclear fuel of a power reactor [16]. In case of abnormal conditions, codes of transient thermal-hydraulics were developed particularly for the safety analysis of power reactors [17], [18]. Some codes

were also developed for analyses of research reactors [19]–[22]. These codes were used to calculate the reactor parameters and for safety analyses. A lot of the reactor parameters cannot be measured experimentally. Validated codes are useful for the prediction of the parameters.

Recent development of 3D virtual reality (VR) technology has pushed its application to improve the effectiveness and efficiency of computer-based simulation tools [23]–[25]. Three basic features of immersion, interaction, and imagination of the VR technology enhance the improvements [26]. Its application in the nuclear field as an education and training tool stimulates a real-like experience without the potential of critical radiation exposure [27]. It is also used for understanding the physical constraints before decommissioning a research reactor. The complex behavior of a nuclear reactor plant during emergency conditions was studied by using a virtual nuclear power plant [28]. The environment of radiation sources and its shielding walls was built based on VR to give the experiences of the beginners and non-expert personnel in handling the radiation sources [29]. A virtual reactor laboratory was also developed in Bangladesh to provide distance learning of the reactor [30].

Kartini research reactor, which belongs to the National Research and Innovation Agency of Indonesia, has been dedicated to nuclear reactor education and training for more than three decades [31]. It covers understanding reactor physics, reactor kinetics, and reactor operation. Furthermore, an online platform called Internet reactor laboratory (IRL) based on the reactor has been developed to provide distance learning of the reactor. These educational activities, however, are performed based on the operation of the real reactor, which lacks conducting a course of reactor operation in case of abnormal or emergency conditions. It is possible to be simulated through a simulation.

A reactor simulator is unique for each reactor. A code-based Kartini research reactor simulator was developed to enable the courses related to emergency conditions [32]. The simulator is intended to have functioned as both a computer-based simulation tool on reactor physics and a code for safety analysis. However, improvement of this simulator is necessary due to a large error in the power data calculation. This current study focuses on code improvement by considering the calculations of control rod worth and temperature reactivity feedbacks and optimizing the neutronic parameters of the delayed neutron fraction, the conduction radial heat transfer coefficient, and the hydraulic diameter. A recent study of experimental-based thermohydraulic analysis of the Kartini research reactor shows interesting results in finding the three stages of heat transfer from the fuel to the coolant. This results in a novel correction factor to quantify the influence of coolant flow on the fuel temperature [33]. The results might be useful for validation of the recent code. The improved code might be further developed by integrating it with the recent IRL and applying the VR to get an immersive distance learning of the reactor. In this research, an early development of 3D virtual reality model is carried out to create an initial immersive IRL platform based on the actual reactor and the simulator.

II. MATERIALS AND METHOD

A. Description of Kartini Reactor

Kartini research reactor is a water-cooled TRIGA Mark-II reactor with an open pool tank. It was designed with thermal power of 250 kWth but was allowed by the Nuclear Energy Regulatory Agency (BAPETEN) to be operated at rated power of 100 kWth. The core characteristics are shown in Table I. It comprises 68 fuel rods with three control rods of safety, shim, and regulating rods. The outside diameter of the fuel is 35.60 mm, surrounded by cladding with a thickness of 0.5 mm. Fig. 1 shows the arrangement of the Kartini reactor. The core diameter is 1.97 m, located at the bottom of the pool tank. It is 4.85 m under the coolant surface of the pool. A passive core coolant flow cools the core. However, an active coolant system is available to circulate hot water, passing two heat exchangers of a flat type and cylinder heat exchangers. This coolant circulation does not affect the core coolant flow. At rated power of 100 kWth, the bulk temperature of the coolant is about 40 °C. The water volume in the tank is so large that the operation of the coolant system does not influence the bulk temperature significantly.

TABLE I
SPECIFICATION OF THE KARTINI REACTOR CORE [32]

Parameter	Value
Thermal power (kW)	100.00
Core pressure (bar)	1.013
Active core height (mm)	380
Fuel rod number	68
Outside diameter of the fuel (mm)	35.60
The fuel gap (mm)	0.20
Outside diameter of the cladding (mm)	37
Hydraulic diameter (mm)	20.976
Cladding thermal conductivity (W/m.K)	16.2
Fuel gap conductivity (W/m.K)	1721

B. Method

The calculation code is built by using Fortran. The code development focuses on the reactor part with boundaries of passive coolant flow and constant reactor pressure of 1 atm. The passive coolant flow is assumed to be one kg/s. The calculation model of neutronic and thermal hydraulics in the reactor is shown in Fig. 2. Three parts are considered in the calculation. The first part is the core, which consists of numerically thirty-six nodes (meshes). The second part is the upper compartment above the core, and the third part is the lower compartment below the core with ten nodes, respectively. The flowchart of the calculation code is shown in Fig. 3. Control rod position and reactivity are taken as the inputs. Besides normal operation, an emergency condition is assumed to happen through a case of reactivity insertion accident, in which the reactivity is increased suddenly due to a control rod ejection. In this study, the excess reactivity of 1.11 \$ is assumed to happen, referring to another similar reactor [4].

The code calculation uses one channel method by considering the average radial power. Meanwhile, the cosine function is taken to approximate the axial power distribution, as shown in Fig. 4 [34]. This study considers one control rod instead of three control rods. During the reactor operation, safety and shim control rods are assumed to be at constant positions of 100% and 70%, respectively.

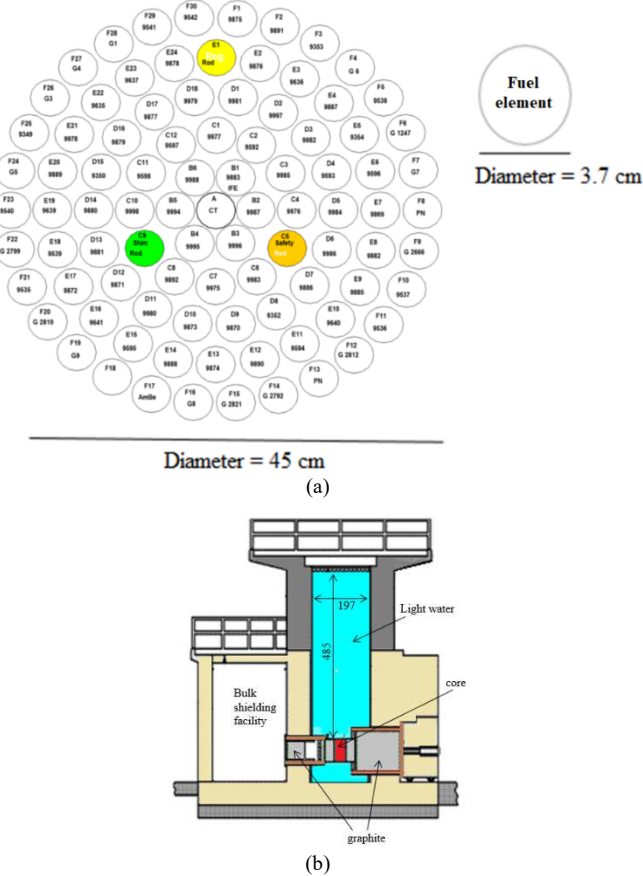


Fig. 1 The Kartini reactor view: (a) Horizontal view of the core; (b) Vertical view of the reactor

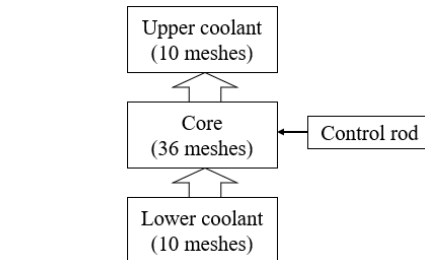


Fig. 2 Model of calculation of the Kartini reactor simulator

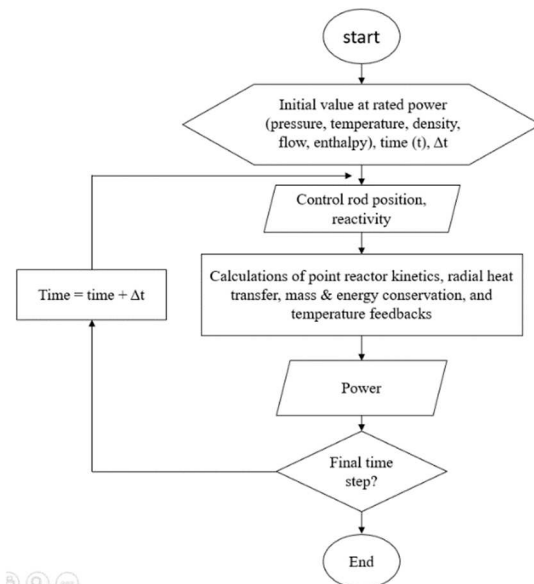


Fig. 3 Flowchart of the calculation code

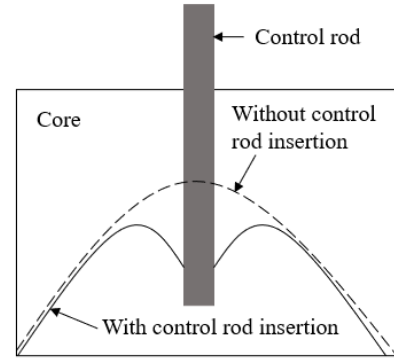


Fig. 4 Power distribution with cosine function approximation [38]

Calculation of neutron flux in the nuclear fuel is described by point reactor kinetic model as shown in Eqs. (1) & (2) [35].

$$\frac{dn(t)}{dt} = S(t) + \frac{(\rho-\beta)}{\Lambda} n(t) + \sum_{i=1}^6 \lambda_i C_i(t) \quad (1)$$

$$\frac{dC_i(t)}{dt} = \frac{\beta_i}{\Lambda} n(t) - \lambda_i C_i(t), \quad i = 1, 2, \dots, 6 \quad (2)$$

Where $n(t)$ is the total number of neutrons at time t , ρ is reactivity, β is delayed neutron fraction, Λ is a neutron life time, λ is the decay constant, and C_i is the number of radioactive precursors. Generated heat due to the fission reaction is assumed to be proportional to the neutron flux. The fraction of delayed neutron (β) refers to that of U-235 fuel as shown in Table II [34].

TABLE II
FRACTION OF DELAYED NEUTRONS FOR U-235 FUEL [34]

Group (i)	Half-time (s)	$\lambda_i(s^{-1})$	β_i
1	55.72	0.0124	0.000215
2	22.72	0.0305	0.001424
3	6.22	0.1115	0.001274
4	2.30	0.301	0.002568
5	0.61	1.138	0.000748
6	0.23	3.01	0.000273

The generated heat produced by the fuel spreads into the coolant through the fuel gap and the cladding wall by conduction heat transfer. Fig. 5 shows the radial heat transfer model from fuel to coolant. Heat conduction is calculated based on Eq. (3) where q is the transferred heat, Z is length of the mesh, K is thermal conductivity, T_a and T_b are temperatures at point a and b with $b > a$, r_a and r_b are radius of point a and b [35].

$$q = \frac{2\pi\Delta Z K}{\ln(r_b/r_a)} (T_a - T_b) \quad (3)$$

Thermal-hydraulic is calculated using mass and energy conservation models, as shown in Eqs. (4-5) where ρ is the coolant density, G is mass flux, h is enthalpy, z is position, t is time, l_f is mesh height, A_f is the outside surface area of the fuel, and q'' is the heat flux. The equations are discretized using the upwind difference and fully implicit schemes [35]. Reactivity feedback due to temperature changes of the fuel and the coolant are considered. A model of the reactivity feedback due to the temperature is shown in Eq. (6), where $\delta\rho$ is the change of reactivity due to the feedback, α_T is the coefficient of temperature reactivity feedback, and δ_T is the average temperature change causing the reactivity feedback.

The coefficient of fuel temperature reactivity feedback is assumed to be constant of $-1.2 \times 10^{-4} \delta\theta/\text{°C}$.

$$\frac{\partial \rho(z,t)}{\partial t} + \frac{\partial G(z,t)}{\partial z} = 0 \quad (4)$$

$$\frac{\partial\{\rho(z,t)h(z,t)\}}{\partial t} + \frac{\partial\{G(z,t)h(z,t)\}}{\partial z} = \frac{1}{A_f} l_f q_n''^k(z, t) \quad (5)$$

$$\partial\rho = \alpha_T \partial T \quad (6)$$

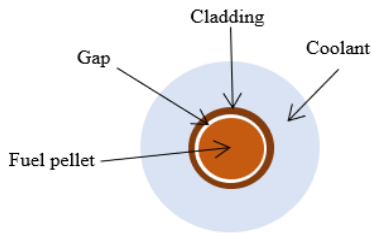


Fig. 5 Radial heat transfer model

3D virtual reality (VR) model is developed using Unity software. Fig. 6 shows the framework of the 3D virtual reality-based platform of the Kartini reactor simulator. The simulator has a function of calculating the reactor data for the given inputs. GUI has a function of a 2D interface for operating the simulator. The 3D virtual reality model allows access to the simulator based on a virtual environment using a VR machine of Oculus.

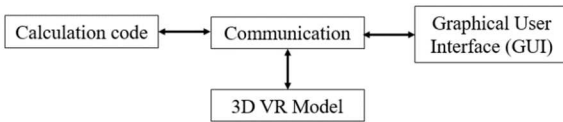


Fig. 6 Framework of 3D VR-based Kartini reactor simulator

III. RESULTS AND DISCUSSION

A graphical user interface (GUI), as shown in Fig. 7, was developed to operate the simulator. It was developed by referring to the GUI used for the operation of the actual Kartini reactor. The regulating control rod (CR) position is set as the input, which the operator can change, while the safety and shim rods are set at a fixed position.

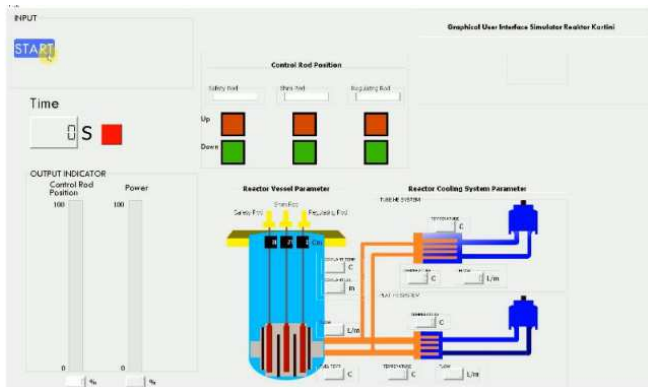


Fig. 7 Graphical user interface of the Kartini reactor simulator

The regulating CR worth is calculated based on experimental data of the CR calibration of the Kartini reactor. The measured data of the CR reactivity as a function of its position is shown in Fig. 8. Withdrawal of the CR results in a

positive reactivity insertion and vice versa. At lower and upper positions, the change of CR position slightly changes the reactivity. At the core's center position, the CR position changes the reactivity significantly. It aligns with the assumption of using the cosine function for the power distribution in the code [34].

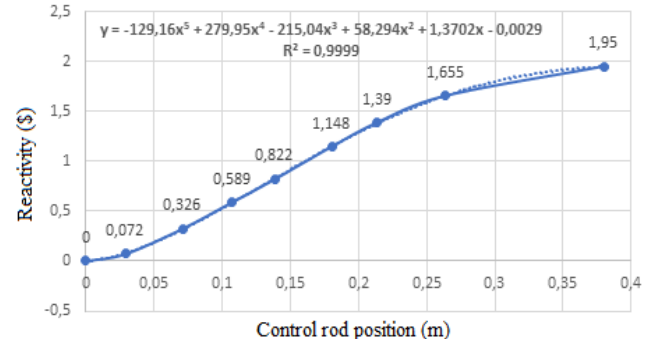


Fig. 8 Experimental data of regulating control rod's reactivity

Figs. 9-12 show the calculation results regarding the insertion of the regulating control rod (CR) by 5% from its rated power position. The decreased position of the CR leads to a negative reactivity insertion of about $-0.38\$$. The power is decreased rapidly within less than 10 s. In turn, it causes a decrease in the coolant bulk temperature. The average density of the coolant is increased.

Meanwhile, the average fuel temperature decreases. Both changes in the coolant average density and the fuel temperature give a positive reactivity feedback that compensates for the control rod insertion, as shown in Fig. 9. Within about 150 s, the total reactivity achieves zero, and the power gets to its stable condition. Since a research reactor has a large negative coefficient of the temperature reactivity feedback, steady state condition of the power could be achieved rapidly. These calculation results show that the Kartini reactor's plant dynamics can be simulated sufficiently.

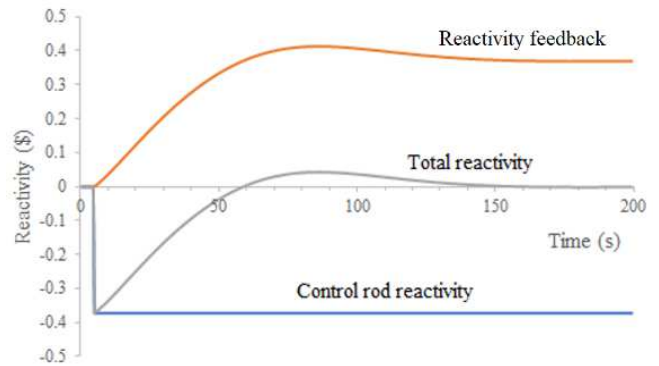


Fig. 9 Change of reactivity due to insertion of CR

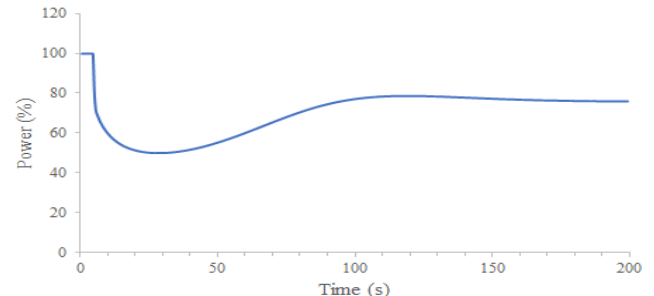


Fig. 10 The power change due to the CR insertion

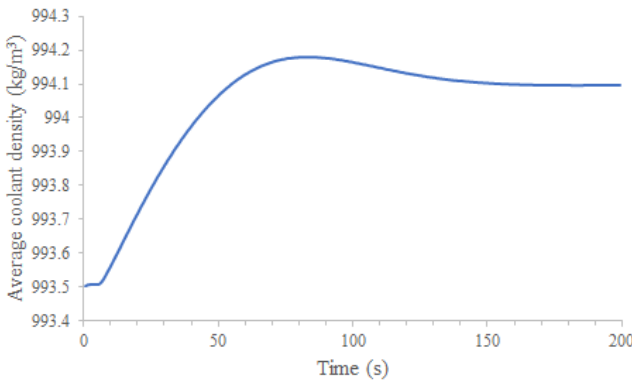


Fig. 11 The density change due to the CR insertion

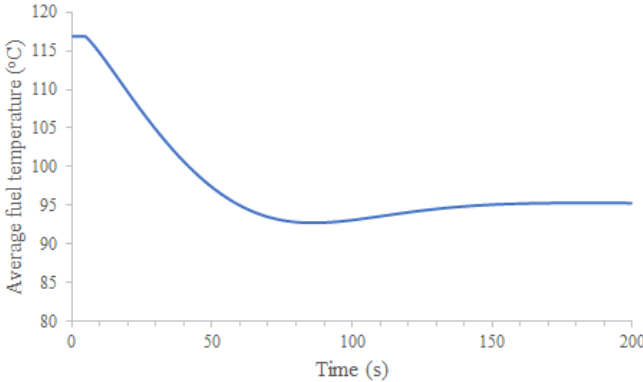


Fig. 12 The fuel temperature change due to the CR insertion

A sensitivity study was carried out to observe the influence of the coefficient change of the temperature reactivity feedback towards the power and the reactivity. The datasheet of the Kartini reactor shows that the coefficient of fuel temperature reactivity feedback is $-1.2 \times 10^{-4} \Delta p/^\circ C$. The coefficient of the coolant density reactivity feedback is taken the same as the previous code [32]. Fig. 13 shows the calculation results regarding the sensitivity simulation. The plant dynamics due to a decrease of the regulating CR position by 5% from its rated power is observed with variation in the coefficient of the fuel temperature reactivity feedback. The decreased position of the CR inserts a negative reactivity and then decreases the power. The more negative the coefficient, the smaller the change of the power. It agrees with the characteristics of the Kartini research reactor, which was designed to have inherent safety by a large coefficient of negative reactivity feedback. The reactor power is not sensitive to perturbation.

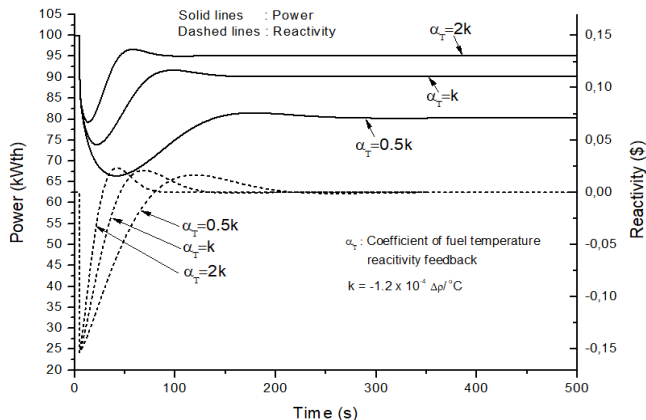


Fig. 13 Variation of coefficient of fuel temperature reactivity feedback

Kartini reactor uses U-235 as the fuel and relatively has a larger delayed neutron fraction than a nuclear power reactor. Fig. 14 shows the influence of delayed neutron fraction change on the power and the reactivity regarding a 5% decrease in the regulating CR position. Kartini reactor has a total delayed neutron fraction of 0.007, which is double that of a nuclear power reactor [35]. The figure shows that a smaller delayed neutron fraction increases the time responses of both the reactivity and the power changes. It means a decrease in the reactor period. Since the Kartini reactor is a research reactor for education and training purposes, it has a high delayed neutron fraction to result in a large reactor period.

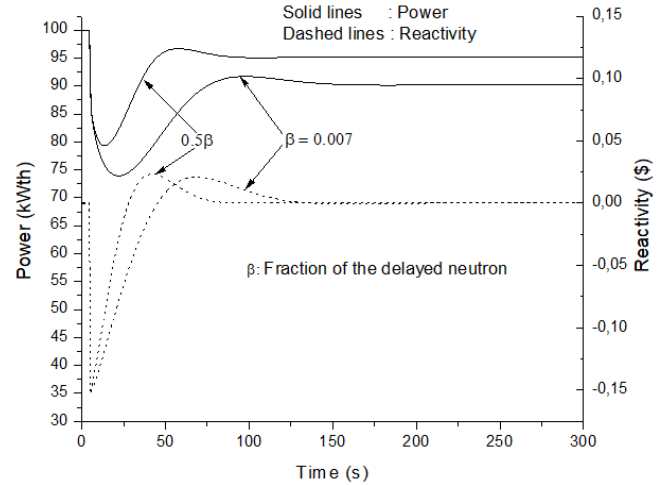


Fig. 14 Variation of delayed neutron fraction

Fig. 15 shows the power changes due to variations of the radial heat conductivity of the cladding. Kartini reactor has a cladding radial heat conductivity of 16.2 W/m.K. The smaller the radial heat conductivity, the smaller the heat transfer from the fuel to the coolant. As a result, the generated heat should be more accumulated in the fuel, increasing the fuel temperature. However, since the Kartini reactor has a low power density, the heat conductivity coefficient variation does not influence the power change significantly [33]. The change of CR position is much dominant in determining the plant behavior.

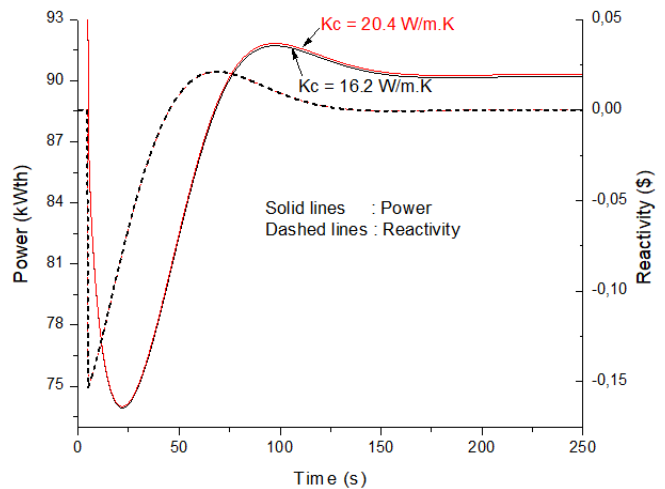


Fig. 15 Variation of cladding thermal conductivity

Hydraulic diameter is an important parameter in the fuel channel. A smaller hydraulic diameter might be meant a smaller volume of the coolant. Based on the fuel channel dimension of the Kartini reactor, its hydraulic diameter is 0.02098 m. Variation of the hydraulic diameter is applied to observe its influence on the power and the reactivity. The simulation results are shown in Fig. 16. It is shown that the smaller hydraulic diameter leads to a higher effect of the reactivity feedback. A half value of the hydraulic diameter results in about 5% higher power at a steady state.

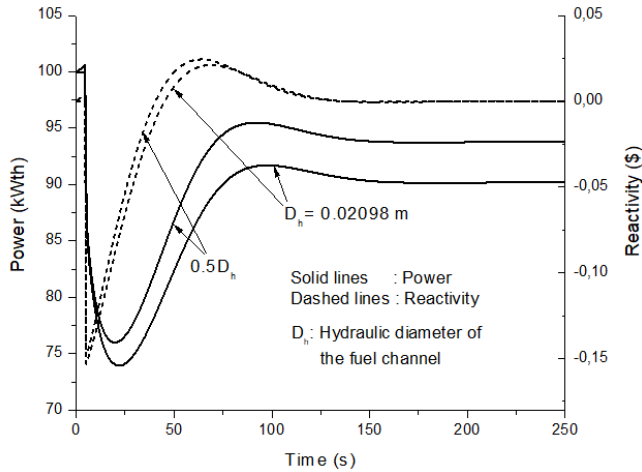


Fig. 16 Variation of hydraulic diameter (D_h)

The power calculations as a function of the CR position are shown in Fig. 17. The calculation is carried out at steady-state conditions referring to a previous study [36]. The simulation data are validated with the experimental data. It is shown that the power calculations using the improved code have a much better agreement to the experimental data than the old code. Since the Kartini reactor's 100% actual power capacity is 250 kWth, the allowed rated power of 100 kWth is achieved at the regulating control rod position of around 41.6%. Therefore, the simulator can be used for data generation of the Kartini reactor's plant dynamics.

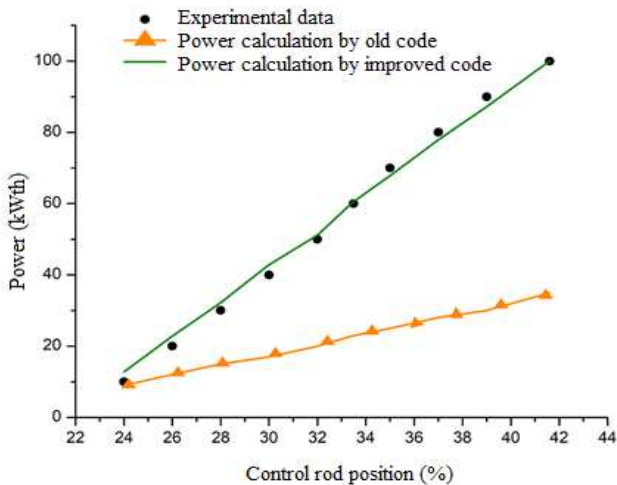


Fig. 17 Power calculation as a function of the CR position

An accident of a CR ejection is simulated as an emergency condition. It inserts a reactivity of 1.11\$, and the simulation

results are shown in Fig. 18. The power is increased rapidly, increasing the fuel temperature to reach about 200 °C. Large negative reactivity feedback, however, mitigates the accident by decreasing the power. A stable condition can be achieved within around 80 s. The research reactor safety analysis satisfies the criterion of considering similar cladding material to that of a power reactor [35], [37]. Given emergency simulation, the generated data of the accident can be used for operator training in abnormal conditions. A lot of alarms might be initiated, and the operator must do the designated procedures for emergency situations so that the reactor can be shut down safely. The features will be the next study of developing the virtual reality-based platform of reactor simulator for education and training.

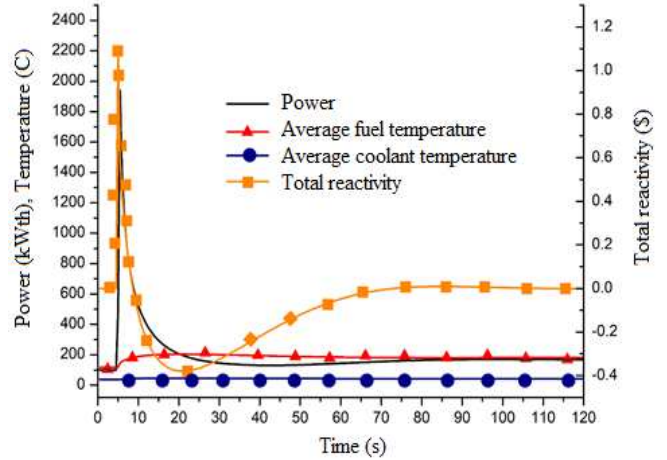


Fig. 18 Simulation of reactivity insertion accident by 1.11 \$

In this study, early development of the 3D VR model of the Kartini reactor was conducted, and the results are shown in Fig. 19. An Oculus VR machine as shown in Fig. 19(a) is used for access the 3D VR models as shown in Fig. 19(b-d). Immersive interaction can be experienced by the user, just like in the real Kartini reactor. However, further development is necessary to improve the immersive feature of the simulator. Operating the simulator which is just like operating the real Kartini reactor, might be achieved through the further development of the 3D VR-based simulator platform.



(a)

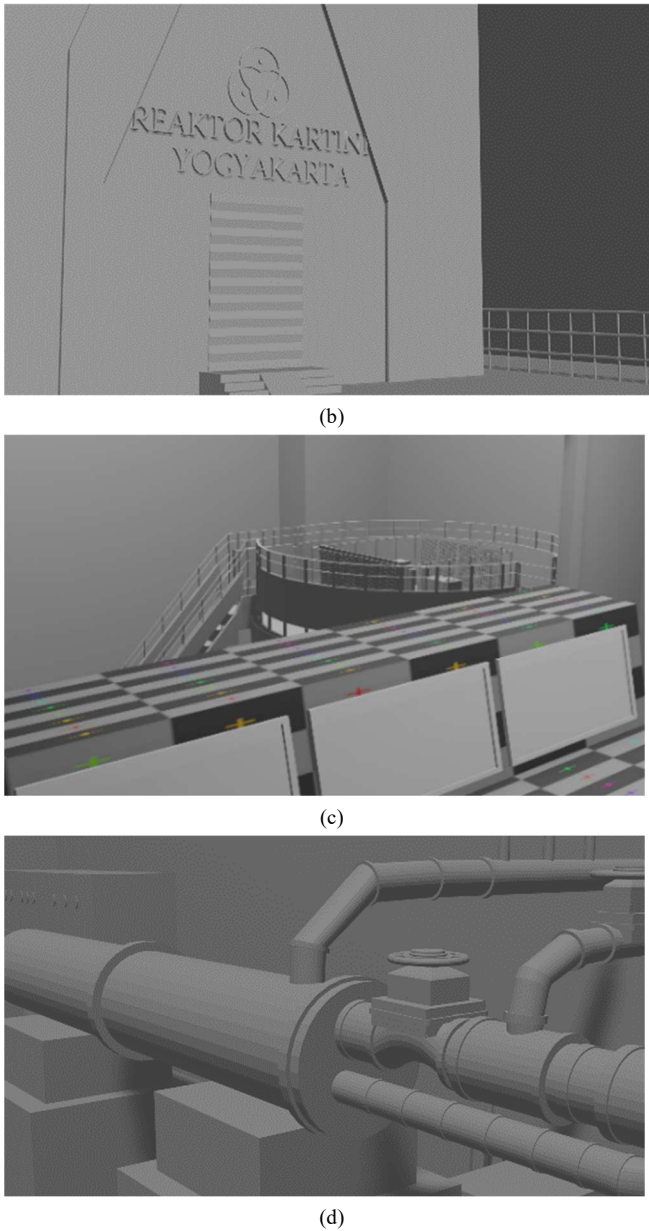


Fig. 19 Model of 3D virtual reality of the Kartini reactor

IV. CONCLUSION

A code-based Kartini research reactor simulator was improved. The power calculation agreed with that of the experimental data of the Kartini reactor operation. Simulation of the reactor dynamics due to insertion and withdrawal of the regulating CR shows satisfactory characteristics as the actual reactor. The sensitivity studies show that the simulator might have the flexibility of modification to be used to simulate another water-cooled research reactor.

The simulator can simulate an abnormal condition of excess reactivity accident, and the maximum cladding temperature safety criterion is satisfied. In the future study, the accident data might be used to initiate a lot of alarm which force the trained operator to strictly do the designated safety procedures to bring the reactor in safe condition.

An early interactive and immersive reactor teaching tool based on 3D VR model was developed. However, further development of the 3D VR model should be carried out to enhance the effectiveness and efficiency of education and

training by using the simulator. Integration among the Kartini reactor simulator, the reactor 3D VR model, and the recent existing facility of the internet reactor laboratory will be interesting further development to provide a facility for nuclear reactor education and training with features of both remote and immersive.

ACKNOWLEDGMENT

The authors thank the Ministry of Science and Technology of Indonesia for funding this research through the Program of INSINAS 2020-2021 with funding no. 04/INS-1/PPK/E4/2020. We are grateful to Prof. Yoshiaki Oka from Waseda University, who taught the first author about code development while studying.

REFERENCES

- [1] M. Tsuboi *et al.*, “Disaster-related deaths after the Fukushima Daiichi nuclear power plant accident - Definition of the term and lessons learned,” *Environ. Adv.*, vol. 8, no. September 2021, p. 100248, 2022, doi: 10.1016/j.envadv.2022.100248.
- [2] G. R. Skillman and J. L. Rempe, “The Three Mile Island Unit 2 Accident,” *Encycl. Nucl. Energy*, pp. 17–29, 2021.
- [3] D. Holiaka, S. Fesenko, V. Kashparov, V. Protsak, S. Levchuk, and M. Holiaka, “Effects of radiation on radial growth of Scots pine in areas highly affected by the Chernobyl accident,” *J. Environ. Radioact.*, vol. 222, no. May, p. 106320, 2020, doi: 10.1016/j.jenvrad.2020.106320.
- [4] K. A. Jordan, D. Springfels, and D. Schubring, “Modern design and safety analysis of the University of Florida Training Reactor,” *Nucl. Eng. Des.*, vol. 286, pp. 89–93, 2015, doi: 10.1016/j.nucengdes.2015.01.019.
- [5] J. Alnaqbi, D. Hartanto, R. Alnuaimi, M. Imron, and V. Gillette, “Static and transient analyses of Advanced Power Reactor 1400 (APR1400) initial core using open-source nodal core simulator KOMODO,” *Nucl. Eng. Technol.*, vol. 54, no. 2, pp. 764–769, 2022, doi: 10.1016/j.net.2021.08.012.
- [6] B. Cui and J. Jiang, “Development of an engineering simulator for a physical component based nuclear process control test facility,” *Simul. Model. Pract. Theory*, vol. 71, pp. 83–101, 2017, doi: 10.1016/j.simpat.2016.11.006.
- [7] Y. Zhao and C. Smidts, “A method for systematically developing the knowledge base of reactor operators in nuclear power plants to support cognitive modeling of operator performance,” *Reliab. Eng. Syst. Saf.*, vol. 186, no. December 2018, pp. 64–77, 2019, doi: 10.1016/j.ress.2019.02.014.
- [8] A. T. Bouma, Q. J. Wei, J. E. Parsons, J. Buongiorno, and J. H. Lienhard, “Energy and water without carbon: Integrated desalination and nuclear power at Diablo Canyon,” *J. Appl. Energy*, vol. 323, p. 119612, 2022.
- [9] M. Ho, E. Obbard, P. A. Burr, and G. Yeoh, “A review on the development of nuclear power reactors,” *Energy Procedia*, vol. 160, no. 2018, pp. 459–466, 2019, doi: 10.1016/j.egypro.2019.02.193.
- [10] W. S. Kim, S. H. Hong, H. S. Choi, S. R. Choi, and D. J. Euh, “Design and validation of a fuel assembly simulator for PGSR reactor flow distribution test facility,” *Nucl. Eng. Des.*, vol. 356, no. May, p. 110353, 2020, doi: 10.1016/j.nucengdes.2019.110353.
- [11] J. Wu *et al.*, “A novel concept for a molten salt reactor moderated by heavy water,” *Ann. Nucl. Energy*, vol. 132, pp. 391–403, 2019, doi: 10.1016/j.anucene.2019.04.043.
- [12] J. Wu, C. Yu, C. Zou, G. Jia, X. Cai, and J. Chen, “Influences of reprocessing separation efficiency on the fuel cycle performances for a Heavy Water moderated Molten Salt Reactor,” *Nucl. Eng. Des.*, vol. 380, no. April, p. 111311, 2021, doi: 10.1016/j.nucengdes.2021.111311.
- [13] M. Imron, “Development and verification of open reactor simulator ADPRES,” *Ann. Nucl. Energy*, vol. 133, pp. 580–588, 2019, doi: 10.1016/j.anucene.2019.06.049.
- [14] J. Malec, D. Toškan, and L. Snoj, “PC-based JSI research reactor simulator,” *Ann. Nucl. Energy*, vol. 146, p. 107630, 2020, doi: 10.1016/j.anucene.2020.107630.
- [15] S. Lyu, D. Lu, and D. Sui, “Neutronics benchmark analysis of the EBR-II SHRT-45R with SAC-3D,” *Nucl. Eng. Des.*, vol. 364, no. May, p. 110679, 2020, doi: 10.1016/j.nucengdes.2020.110679.

- [16] P. Suk, O. Chvála, I. G. Maldonado, and J. Rataj, "Evaluation of end of cycle plutonium isotopic content in a VVER-1000 reactor using a 3D full-core simulator," *Nucl. Eng. Des.*, vol. 377, no. August 2020, p. 111133, 2021, doi: 10.1016/j.nucengdes.2021.111133.
- [17] Y. Yu *et al.*, "Research and development of a transient thermal-hydraulic code for system safety analysis of sodium cooled fast reactor," *Ann. Nucl. Energy*, vol. 152, p. 107841, 2021, doi: 10.1016/j.anucene.2020.107841.
- [18] T. Meng, K. Cheng, F. Zhao, C. Xia, and S. Tan, "Dynamic simulation of the gas-cooled space nuclear reactor system using SIMCODE," *Ann. Nucl. Energy*, vol. 159, p. 108293, 2021, doi: 10.1016/j.anucene.2021.108293.
- [19] M. Alqahtani, A. Buijs, and S. E. Day, "Experimental measurement and Monte Carlo code simulation of the gamma heating at different irradiation sites in a nuclear research reactor," *Nucl. Eng. Des.*, vol. 364, no. May, p. 110690, 2020, doi: 10.1016/j.nucengdes.2020.110690.
- [20] T. Liu, Z. Wu, C. Lu, and R. P. Martin, "A best estimate plus uncertainty safety analysis framework based on RELAP5-3D and RAVEN platform for research reactor transient analyses," *Prog. Nucl. Energy*, vol. 132, no. December 2020, p. 103610, 2021, doi: 10.1016/j.pnucene.2020.103610.
- [21] S. Safaei Arshi, M. Amin Mozafari, A. Jozvaziri, and S. M. Mirvakili, "Investigation of safety aspects during steady state operation of Tehran research reactor fuel test loop," *Prog. Nucl. Energy*, vol. 140, no. December 2020, p. 103895, 2021, doi: 10.1016/j.pnucene.2021.103895.
- [22] K. O. Kim, G. Roh, and B. Lee, "Neutronic performance of the hybrid-low power research reactor for education and neutron applications," *Ann. Nucl. Energy*, vol. 158, p. 108272, 2021, doi: 10.1016/j.anucene.2021.108272.
- [23] I. Kovar, "Use of virtual reality as a tool to overcome the post-traumatic stress disorder of pensioners," *Int. J. Adv. Sci. Eng. Inf. Technol.*, vol. 9, no. 3, pp. 841–848, 2019, doi: 10.18517/ijaseit.9.3.8245.
- [24] J. D. Abril, O. Rivera, O. I. Caldas, M. F. Maledoux, and O. F. Avilés, "Serious game design of virtual reality balance rehabilitation with a record of psychophysiological variables and emotional assessment," *Int. J. Adv. Sci. Eng. Inf. Technol.*, vol. 10, no. 4, pp. 1519–1525, 2020, doi: 10.18517/ijaseit.10.4.10319.
- [25] Z. Guo *et al.*, "Applications of virtual reality in maintenance during the industrial product lifecycle: A systematic review," *J. Manuf. Syst.*, vol. 56, no. May 2019, pp. 525–538, 2020, doi: 10.1016/j.jmsy.2020.07.007.
- [26] S. Qin, Q. Wang, and X. Chen, "Application of virtual reality technology in nuclear device design and research," *Fusion Eng. Des.*, vol. 161, no. March, p. 111906, 2020, doi: 10.1016/j.fusengdes.2020.111906.
- [27] L. Gabcan, A. S. M. Alves, and P. F. Frutuoso e Melo, "3D simulation model of water infiltration for radioactive waste on a virtual reality Environment: An application to the Abadia de Goiás repository," *Ann. Nucl. Energy*, vol. 140, p. 107265, 2020, doi: 10.1016/j.anucene.2019.107265.
- [28] Y. Wu, "Development and application of virtual nuclear power plant in digital society environment," *Int. J. Energy Res.*, vol. 43, no. 4, pp. 1521–1533, 2019, doi: 10.1002/er.4378.
- [29] K. Hagita, Y. Kodama, and M. Takada, "Simplified virtual reality training system for radiation shielding and measurement in nuclear engineering," *Prog. Nucl. Energy*, vol. 118, no. August 2019, p. 103127, 2020, doi: 10.1016/j.pnucene.2019.103127.
- [30] A. Das, M. S. Hossain, M. K. A. Rabby, and R. Barman, "Virtual reactor laboratory integrated with cyber security from Bangladesh perspective," *Int. J. Adv. Nucl. React. Des. Technol.*, vol. 3, no. October 2021, pp. 184–193, 2021, doi: 10.1016/j.jandt.2021.09.005.
- [31] S. Syarip and P. I. Wahyono, "Experience in nuclear reactor physics laboratory exercises using Kartini research reactor," *J. Phys. Conf. Ser.*, vol. 1157, no. 3, 2019, doi: 10.1088/1742-6596/1157/3/032002.
- [32] Sutanto, A. M. D. Suryana, and Syarip, "Development of Kartini Reactor Code to Support Nuclear Training Center and Safety Analysis," *2018 4th Int. Conf. Sci. Technol.*, vol. 1, pp. 1–6, 2018.
- [33] B. Riyono, R. Pulungan, A. Dharmawan, and A. R. Antariksawan, "Experimental investigation on the thermohydraulic parameters of Kartini research reactor under variation of the primary pump flow," *Appl. Therm. Eng.*, vol. 213, p. 118674, 2022.
- [34] US Department of Energy, "Doe Fundamentals Handbook Nuclear Physics Volume 1 of 2," *Nucl. Phys.*, vol. 1, no. January 1993, p. 36, 2003.
- [35] Y. Oka, S. Koshizuka, Y. Ishiwatari, and A. Yamaji, *Super Light Water Reactors and Super Fast Reactors*. Springer, 2010.
- [36] A. S. Ványi *et al.*, "Steady-state neutronic measurements and comprehensive numerical analysis for the BME training reactor," *Ann. Nucl. Energy*, vol. 155, 2021, doi: 10.1016/j.anucene.2021.108144.
- [37] M. K. Rowinski, J. Zhao, T. J. White, and Y. C. Soh, "Safety analysis of Super-Critical Water Reactors—A review," *Prog. Nucl. Energy*, vol. 106, no. February, pp. 87–101, 2018, doi: 10.1016/j.pnucene.2018.03.002.